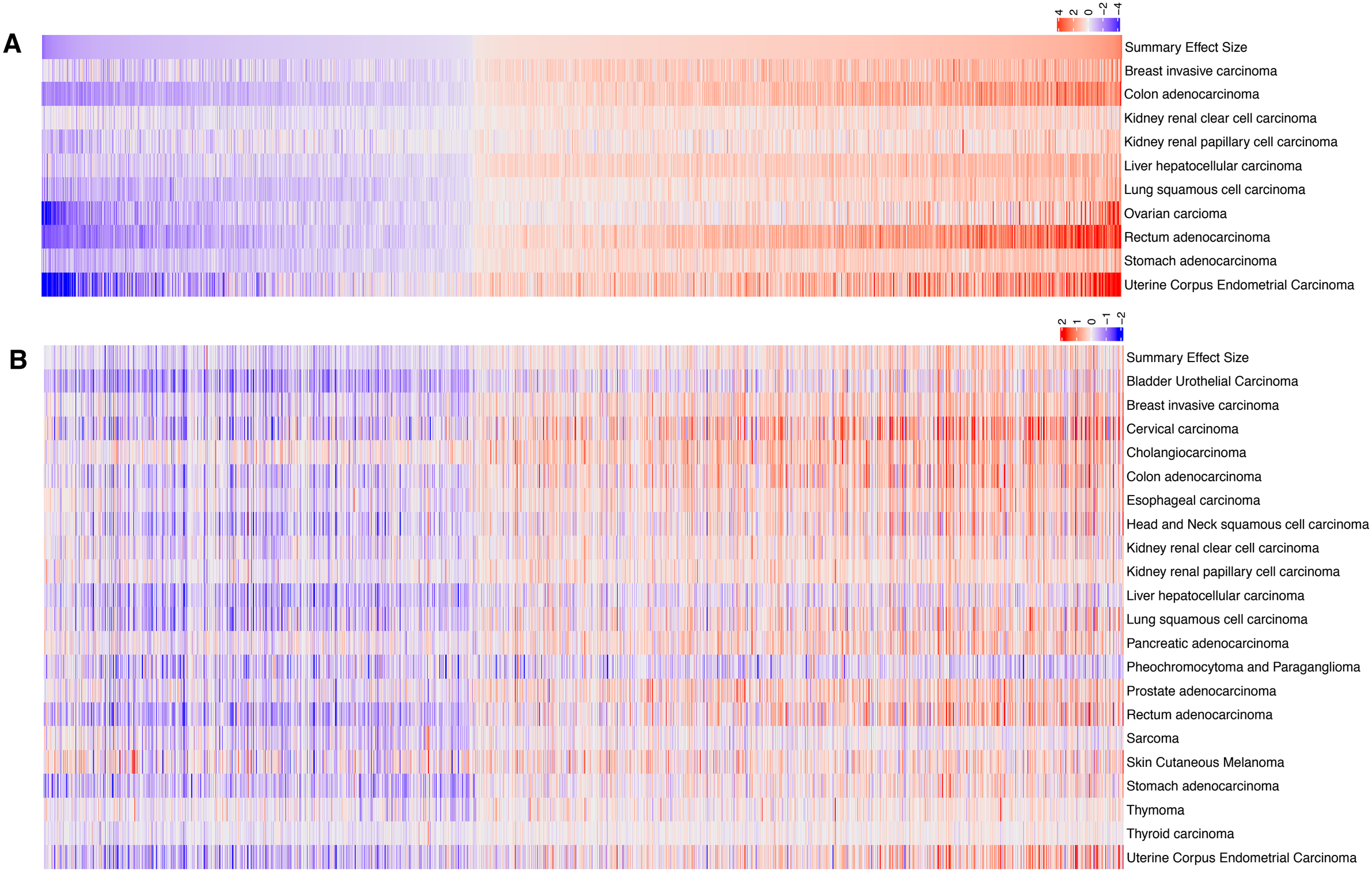

Supplemental Figure 1. 1,801 differentially methylated genes (1,081 hyper- and 720 hypomethylated, FDR < 5%) across all cancers. Top row indicates the summary effect size across all cancers in **(A)** the discovery data using the Illumina 27 platform and **(B)** validation data on the Illumina 450 platform. Gene order is maintained between **(A)** and **(B)**.

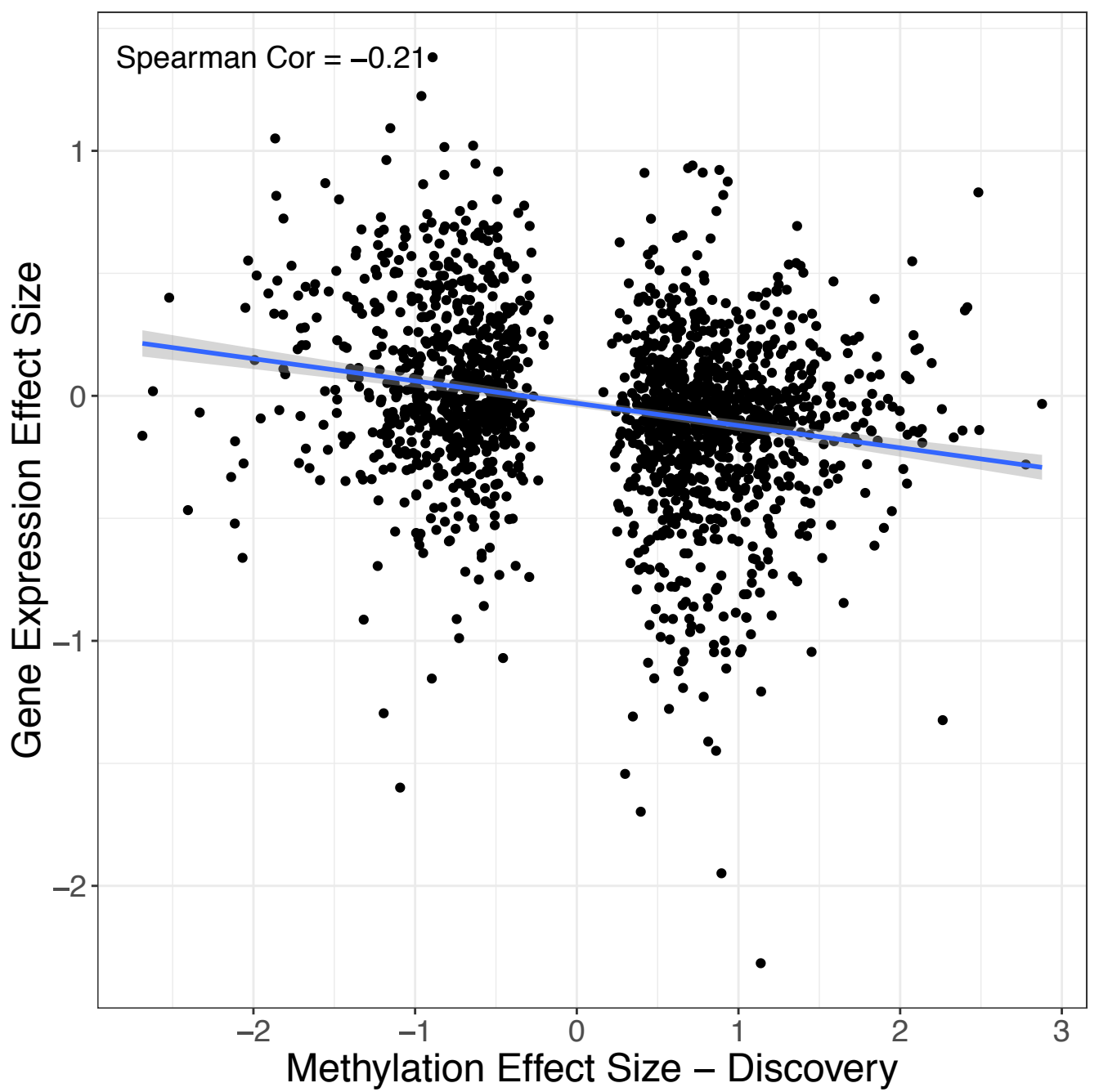

Supplemental Figure 2. Spearman correlation between the discovery methylation effect size and gene expression effectsize across the 1,801 differentially methylated genes

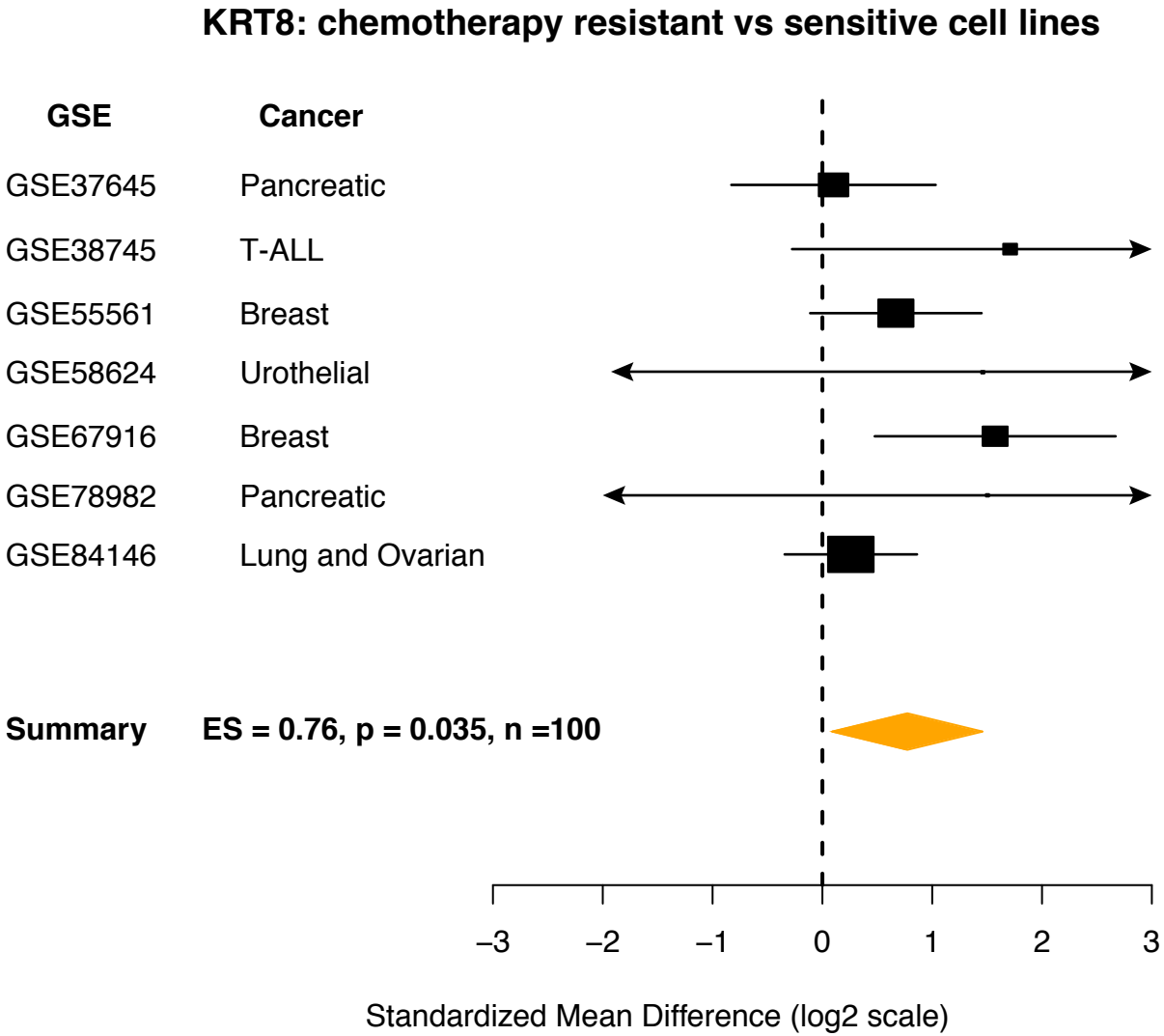

Supplemental Figure 3. Expression of KRT8 in chemotherapy resistant cancer cell lines compared to chemotherapy sensitive cell lines in the same tissue across seven independent datasets. ES = Effect size.

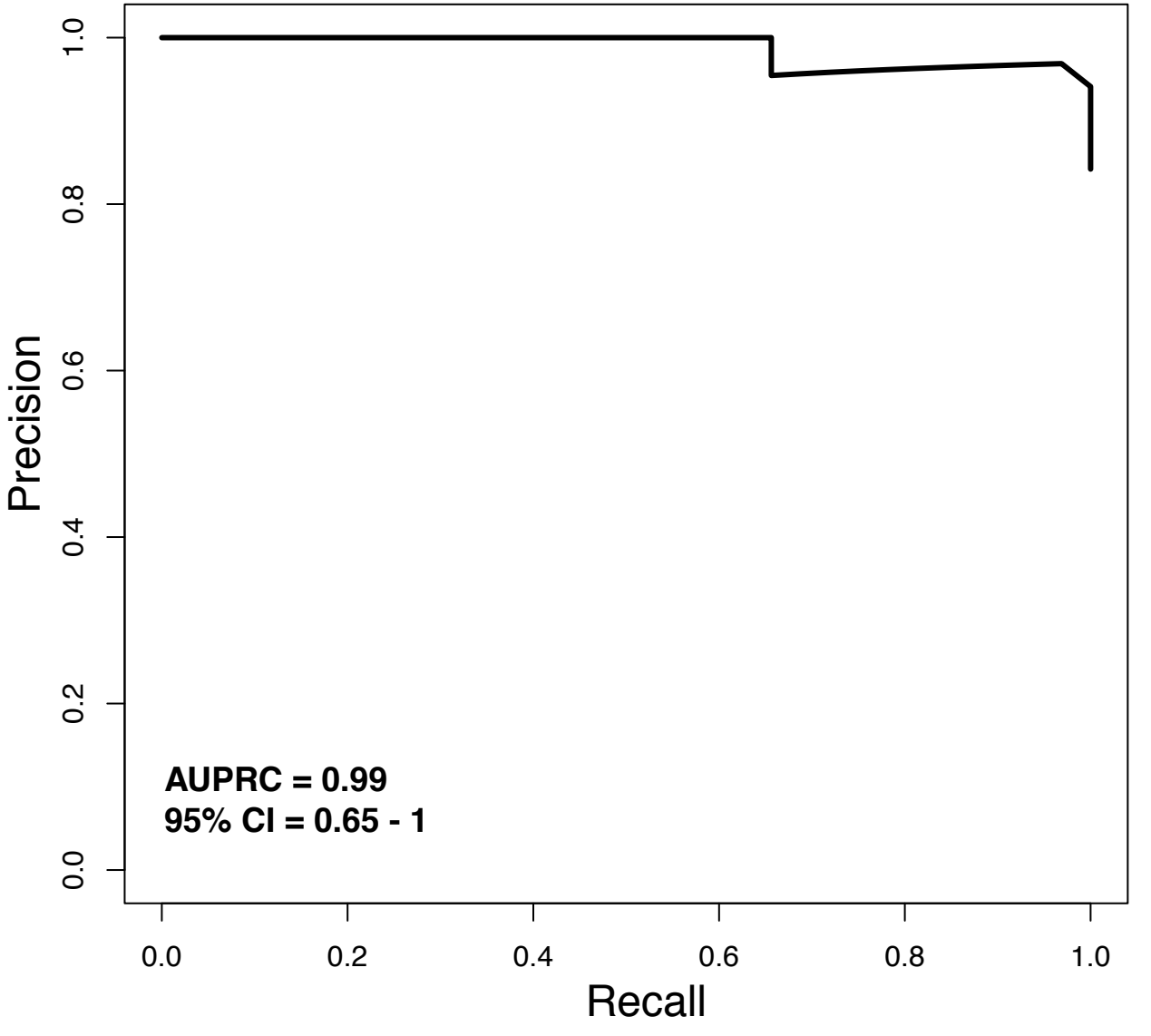

Supplemental Figure 4. Precision-Recall curve for desciminating pancreatic cancer patients (n = 32) from healthy controls (n = 6) by serum KRT8 as measured by ELISA.

Supplemental Table 1. Reactome pathway analysis of 100 most KRT8-correlated and anticorrelated genes. Correlations were determined from expression levels within single cells.

Upregulated	Pathway	p.Geomean	Stat mean	P val	qval	set size	exp1
	GO:0034220 ion transmembrane transport	0.021	2.185	0.021	0.921	15.000	0.021
	GO:0007017 microtubule-based process	0.030	1.975	0.030	0.921	15.000	0.030
	GO:0006091 generation of precursor metabolites and energy	0.039	1.884	0.039	0.921	12.000	0.039
	GO:0000226 microtubule cytoskeleton organization	0.040	1.866	0.040	0.921	10.000	0.040
	GO:0045088 regulation of innate immune response	0.062	1.633	0.062	0.921	12.000	0.062
	GO:0034097 response to cytokine stimulus	0.064	1.544	0.064	0.921	31.000	0.064
Down							
	GO:0007155 cell adhesion	0.006	-2.554	0.006	0.822	49.000	0.006
	GO:0022610 biological adhesion	0.006	-2.554	0.006	0.822	49.000	0.006
	GO:0030155 regulation of cell adhesion	0.007	-2.674	0.007	0.822	14.000	0.007
	GO:0016337 cell-cell adhesion	0.009	-2.497	0.009	0.822	19.000	0.009
	GO:0051336 regulation of hydrolase activity	0.027	-1.956	0.027	0.822	42.000	0.027
	GO:0006790 sulfur compound metabolic process	0.045	-1.810	0.045	0.822	10.000	0.045

Supplementary Table 2. Correlation of six genes with KRT8 expression in bulk tissue microarrays

Cancer	Gene Name	effectSize	effectSizeStandardError	effectSizePval	effectSizeFDR	# Studies
Lung adenocarcinoma	GPX2	0.85825435	0.10343277	1.06E-16	8.33E-16	12
	SFN	1.73484346	0.24509068	1.46E-12	7.97E-12	12
	GSTP1	0.36090358	0.11225354	0.0013041	0.0025582	12
	COX6A1	0.38921725	0.16041534	0.01525326	0.02462262	11
	PRDX5	-0.2398083	0.12480822	0.05467952	0.07900236	10
	TXNRD1	0.20785324	0.12609836	0.09928248	0.13484462	12
Breast invasive carcinoma	GPX2	-0.2375308	0.04801474	7.54E-07	1.35E-05	11
	GSTP1	-0.3034343	0.08920859	0.00067041	0.00381338	11
	SFN	0.61918602	0.25434585	0.01491545	0.04712083	9
	COX6A1	0.34303382	0.19992861	0.08620203	0.19004273	10
	PRDX5	0.06965973	0.15040264	0.64325327	0.78503691	10
	TXNRD1	-0.013877	0.09478392	0.88360029	0.937214	11
Colon adenocarcinoma	TXNRD1	0.29526367	0.14820284	0.04633878	0.57457234	9
	SFN	0.16939059	0.14314671	0.23667617	0.81649353	9
	COX6A1	0.21129821	0.18870124	0.26282031	0.83222568	10
	GSTP1	0.11125449	0.18337014	0.54403616	0.93600853	9
	GPX2	-0.0618429	0.1610988	0.70106622	0.96388548	10
	PRDX5	-0.0106303	0.1627399	0.9479186	0.99373678	7
Pancreatic carcinoma	SFN	1.55433781	0.15874762	1.23E-22	5.72E-20	11
	GSTP1	1.24803455	0.19765895	2.72E-10	1.26E-08	11
	GPX2	1.09113993	0.17950857	1.21E-09	4.79E-08	12
	TXNRD1	0.79114389	0.21840454	0.00029191	0.00173964	12
	PRDX5	0.78212231	0.22006658	0.00037938	0.00214582	11
	COX6A1	0.17429096	0.16489239	0.2905124	0.40571164	11
Ovarian carcioma	SFN	1.60402136	0.26433707	1.29E-09	1.11E-07	12
	GSTP1	1.33878562	0.46126096	0.00370259	0.0316481	12
	COX6A1	0.59523921	0.23225486	0.01038107	0.06663287	12
	TXNRD1	-0.4461765	0.23997164	0.06298629	0.22142444	12
	GPX2	-0.2316358	0.18909074	0.22057584	0.46257419	12
	PRDX5	0.17328605	0.39255309	0.65889926	0.81042429	10

Supplementary Table 3. Demographic information for the adenocarcinoma patients profiled by tissue microarray.

n	294
Grade (%)	
well	39 (13.3)
moderate	167 (56.8)
poor	82 (27.9)
undifferentiated	1 (0.3)
not stated	4 (1.7)
Age (mean (SD))	67.70 (10.49)
Sex = male (%)	135 (45.9)
Primary tumor size (mean (SD))	3.45 (2.00)
Subtype (%)	
Adenocarcinoma	228 (77.6)
Squamous cell	66 (22.4)
Stage (mean (SD))	1.64 (0.76)

Supplementary Table 4. Demographic information for the 176 patients with pancreatic cancer.

Characteristic	Overall
n	176
Age (mean (SD))	64.85 (10.77)
Male (%)	96 (54.5)
Stage (%)	
i	1 (0.6)
ia	5 (2.8)
ib	15 (8.5)
iia	28 (15.9)
iib	117 (66.5)
iii	3 (1.7)
iv	4 (2.3)
not reported	3 (1.7)
Days observed (mean	570.65 (478.36)
FPKM (mean (SD))	386.77 (218.16)
Died (%)	92 (52.3)

Supplementary Figure 5. Demographic information on 32 patients with pancreatic cancer.

Patients' age (years), mean (range)	69 (43 - 85)
Female, *n* (%)	12 (38)
Tumor grade, *n* (%)	
Well differentiated	7 (22)
Moderately differentiated	19 (59)
Poorly differentiated	6 (19)
Lymph node status, *n* (%)	
Positive	16 (50)
Negative	16 (50)
Resection margin, *n* (%)	
Positive	10 (31)
Negative	22 (69)
Tumor size (cm), median (range)	3.80 (1.10-6.00)
Bilirubin (mg/dL), mean (range)	0.65 (0.5-1.3)
CA19-9 (U/ml), mean (range)	26059 (1-780486)

Supplementary Table 6

Dataset	Link	Organ
GSE2514	https://www.ncbi.nlm.nih.gov/geo/query/acc.cgi?acc=GSE2514	Lung
GSE10072	https://www.ncbi.nlm.nih.gov/geo/query/acc.cgi?acc=GSE10072	Lung
GSE12236	https://www.ncbi.nlm.nih.gov/geo/query/acc.cgi?acc=GSE12236	Lung
GSE19188	https://www.ncbi.nlm.nih.gov/geo/query/acc.cgi?acc=GSE19188	Lung
GSE27262	https://www.ncbi.nlm.nih.gov/geo/query/acc.cgi?acc=GSE27262	Lung
GSE30219	https://www.ncbi.nlm.nih.gov/geo/query/acc.cgi?acc=GSE30219	Lung
GSE31210	https://www.ncbi.nlm.nih.gov/geo/query/acc.cgi?acc=GSE31210	Lung
GSE32863	https://www.ncbi.nlm.nih.gov/geo/query/acc.cgi?acc=GSE32863	Lung
GSE43458	https://www.ncbi.nlm.nih.gov/geo/query/acc.cgi?acc=GSE43458	Lung
GSE43767	https://www.ncbi.nlm.nih.gov/geo/query/acc.cgi?acc=GSE43767	Lung
GSE63459	https://www.ncbi.nlm.nih.gov/geo/query/acc.cgi?acc=GSE63459	Lung
GSE75037	https://www.ncbi.nlm.nih.gov/geo/query/acc.cgi?acc=GSE75037	Lung
GSE42568	https://www.ncbi.nlm.nih.gov/geo/query/acc.cgi?acc=GSE42568	Breast
GSE20711	https://www.ncbi.nlm.nih.gov/geo/query/acc.cgi?acc=GSE20711	Breast
GSE15852	https://www.ncbi.nlm.nih.gov/geo/query/acc.cgi?acc=GSE15852	Breast
GSE37751	https://www.ncbi.nlm.nih.gov/geo/query/acc.cgi?acc=GSE37751	Breast
GSE13293	https://www.ncbi.nlm.nih.gov/geo/query/acc.cgi?acc=GSE13293	Breast
GSE22820	https://www.ncbi.nlm.nih.gov/geo/query/acc.cgi?acc=GSE22820	Breast
GSE31448	https://www.ncbi.nlm.nih.gov/geo/query/acc.cgi?acc=GSE31448	Breast
GSE54002	https://www.ncbi.nlm.nih.gov/geo/query/acc.cgi?acc=GSE54002	Breast
GSE4382	https://www.ncbi.nlm.nih.gov/geo/query/acc.cgi?acc=GSE4382	Breast
GSE109169	https://www.ncbi.nlm.nih.gov/geo/query/acc.cgi?acc=GSE109169	Breast
GSE93601	https://www.ncbi.nlm.nih.gov/geo/query/acc.cgi?acc=GSE93601	Breast
MTAB10971	https://www.ncbi.nlm.nih.gov/geo/query/acc.cgi?acc=MTAB10971	Ovarian
MTAB18520	https://www.ncbi.nlm.nih.gov/geo/query/acc.cgi?acc=MTAB18520	Ovarian
MTAB25427	https://www.ncbi.nlm.nih.gov/geo/query/acc.cgi?acc=MTAB25427	Ovarian
MTAB6008	https://www.ncbi.nlm.nih.gov/geo/query/acc.cgi?acc=MTAB6008	Ovarian
MTAB14001	https://www.ncbi.nlm.nih.gov/geo/query/acc.cgi?acc=MTAB14001	Ovarian
MTAB19352	https://www.ncbi.nlm.nih.gov/geo/query/acc.cgi?acc=MTAB19352	Ovarian
MTAB26712	https://www.ncbi.nlm.nih.gov/geo/query/acc.cgi?acc=MTAB26712	Ovarian
GSE66957	https://www.ncbi.nlm.nih.gov/geo/query/acc.cgi?acc=GSE66957	Ovarian
GSE54388	https://www.ncbi.nlm.nih.gov/geo/query/acc.cgi?acc=GSE54388	Ovarian
GSE40595	https://www.ncbi.nlm.nih.gov/geo/query/acc.cgi?acc=GSE40595	Ovarian
GSE37582	https://www.ncbi.nlm.nih.gov/geo/query/acc.cgi?acc=GSE37582	Ovarian
GSE36668	https://www.ncbi.nlm.nih.gov/geo/query/acc.cgi?acc=GSE36668	Ovarian
GSE46234	https://www.ncbi.nlm.nih.gov/geo/query/acc.cgi?acc=GSE46234	Pancreatic
GSE63111	https://www.ncbi.nlm.nih.gov/geo/query/acc.cgi?acc=GSE63111	Pancreatic
GSE62452	https://www.ncbi.nlm.nih.gov/geo/query/acc.cgi?acc=GSE62452	Pancreatic
GSE56560	https://www.ncbi.nlm.nih.gov/geo/query/acc.cgi?acc=GSE56560	Pancreatic
GSE55643	https://www.ncbi.nlm.nih.gov/geo/query/acc.cgi?acc=GSE55643	Pancreatic
GSE43795	https://www.ncbi.nlm.nih.gov/geo/query/acc.cgi?acc=GSE43795	Pancreatic

GSE23397	https://www.ncbi.nlm.nih.gov/geo/query/acc.cgi?acc=GSE23397	Pancreatic
GSE39751	https://www.ncbi.nlm.nih.gov/geo/query/acc.cgi?acc=GSE39751	Pancreatic
GSE28735	https://www.ncbi.nlm.nih.gov/geo/query/acc.cgi?acc=GSE28735	Pancreatic
GSE15932	https://www.ncbi.nlm.nih.gov/geo/query/acc.cgi?acc=GSE15932	Pancreatic
GSE32676	https://www.ncbi.nlm.nih.gov/geo/query/acc.cgi?acc=GSE32676	Pancreatic
GSE22780	https://www.ncbi.nlm.nih.gov/geo/query/acc.cgi?acc=GSE22780	Pancreatic
GSE103512	https://www.ncbi.nlm.nih.gov/geo/query/acc.cgi?acc=GSE103512	Colon
GSE89287	https://www.ncbi.nlm.nih.gov/geo/query/acc.cgi?acc=GSE89287	Colon
GSE76855	https://www.ncbi.nlm.nih.gov/geo/query/acc.cgi?acc=GSE76855	Colon
GSE62932	https://www.ncbi.nlm.nih.gov/geo/query/acc.cgi?acc=GSE62932	Colon
GSE68468	https://www.ncbi.nlm.nih.gov/geo/query/acc.cgi?acc=GSE68468	Colon
GSE62321	https://www.ncbi.nlm.nih.gov/geo/query/acc.cgi?acc=GSE62321	Colon
GSE49355	https://www.ncbi.nlm.nih.gov/geo/query/acc.cgi?acc=GSE49355	Colon
GSE39582	https://www.ncbi.nlm.nih.gov/geo/query/acc.cgi?acc=GSE39582	Colon
GSE41328	https://www.ncbi.nlm.nih.gov/geo/query/acc.cgi?acc=GSE41328	Colon
GSE41258	https://www.ncbi.nlm.nih.gov/geo/query/acc.cgi?acc=GSE41258	Colon